Flexible Carrier Loop Design for the Spacecraft Transponding Modem (STM)

J. B. Berner,[1] J. M. Layland,[1] and P. W. Kinman[2]

The best-lock frequency of an idling carrier loop drifts in response to thermal noise at the receiver input. This effect is less for a loop with an imperfect integrator than it is for a loop of the same bandwidth with a perfect integrator. But perfect integration gives better tracking performance. In order to provide mission designers with a choice of loop types, the Spacecraft Transponding Modem (STM) will have a flexible loop filter design that can be programmed for either perfect or imperfect integration.

I. Introduction

The Spacecraft Transponding Modem (STM) will have a second-order carrier loop. A second-order phase-locked loop is one that has a loop filter with first-order transfer function. (The other pole arises in the integration performed by the numerically controlled oscillator.) A first-order loop filter may use either perfect or imperfect integration. The former has been used to good effect in ground-based receivers, such as the Block V Receiver. Deep-space transponders, on the other hand, traditionally have used imperfect integration in the carrier loop. The STM carrier loop filter has a flexible, digital design, which permits either perfect or imperfect integration. STM is the first deep-space transponder to feature such flexibility.

It is well-known that a loop with a perfect integrator offers the better tracking performance [1]. For example, when the arriving carrier has a constant frequency offset, δf, from the best-lock frequency, the loop with a perfect integrator has zero phase error but the loop with an imperfect integrator has a phase error of $2\pi\delta f/(\alpha K)$, where αK is the loop gain.

There is one respect in which a loop with an imperfect integrator is better. When the loop idles (i.e., when noise alone is at the input), the best-lock frequency of the loop will drift less (for a given loop bandwidth) if the loop filter integration is imperfect, rather than perfect. In light of this, a flexible carrier-loop filter implementation has been proposed for STM that accommodates both perfect and imperfect integration. The mission designer can weigh the relative advantages of these two loop filter types and then program the STM accordingly.

---

[1] Communications Ground Systems Section.

[2] Case Western Reserve University, Cleveland, Ohio.

The first section of this article is a review of the STM carrier loop design. More details of this design are available in the principal engineering literature for the STM.[3,4] The second section shows how the best-lock frequency can drift while the carrier loop is idling. The third section explains the flexible loop filter implementation.

II. Review of STM Carrier Loop Design

Within the STM, the received uplink signal is amplified, filtered, downconverted, and sampled. Figure 1 shows the analog front-end. (Not shown is a low-noise amplifier at the very front; although important for good receiver sensitivity, it does not play a role in the analysis that follows.)

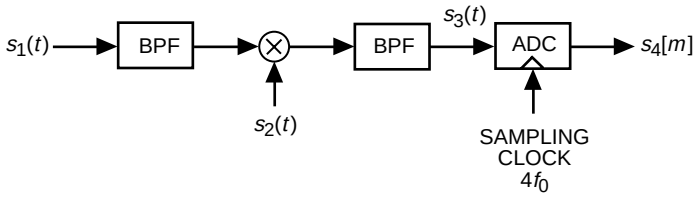

Fig. 1. Analog signal processing in the STM receiver.

The arriving uplink signal ordinarily will comprise a residual carrier and modulation sidebands. Only the residual carrier is of interest here; it is of the form

$$s_1(t) = \sqrt{2P_C}\sin\left(2\pi \times 749 f_0 t + \theta\right) \tag{1}$$

where P_C is the carrier power, f_0 is a convenient unit of measure for frequency, and θ is an implicit function of time. The f_0 equals one-eighth the frequency of the STM reference generator. The uplink carrier is not coherent with the STM reference generator; this fact is modeled by the presence of a time-varying θ in Eq. (1). White noise accompanies $s_1(t)$; its power spectral density is here denoted N_0.

The bandpass filter preceding the mixer rejects image-band noise. The local oscillator is of the form

$$s_2(t) = \sqrt{2}\cos\left(2\pi \times 736 f_0 t + \hat{\theta}\right) \tag{2}$$

When the loop is in lock, $\hat{\theta}$ approximates θ, and the loop phase error,

$$\phi = \theta - \hat{\theta} \tag{3}$$

is approximately zero. The desired mixer product is of the form

$$s_3(t) = \sqrt{P_C}\sin\left(2\pi \times 13 f_0 t + \phi\right) \tag{4}$$

White noise having power spectral density $N_0/2$ accompanies $s_3(t)$.

---

[3] *Spacecraft Transponding Modem (STM) Transponder ASIC Specifications*, CS-517513 (internal document), Jet Propulsion Laboratory, Pasadena, California, May 18, 1998.

[4] *Prototype Spacecraft Transponding Modem (STM) Preliminary Design Review*, (internal document), Jet Propulsion Laboratory, Pasadena, California, June 2, 1998.

In the two-way coherent mode, the STM exciter produces a downlink carrier of the form

$$\sin\left[2\pi \times 880 f_0 t + \frac{880}{749}\hat{\theta}\right] = \sin\left[\frac{880}{749}\left(2\pi \times 749 f_0 t + \hat{\theta}\right)\right] \tag{5}$$

for 8400 to 8500 MHz (X-band) or

$$\sin\left[2\pi \times 3344 f_0 t + \frac{3344}{749}\hat{\theta}\right] = \sin\left[\frac{3344}{749}\left(2\pi \times 749 f_0 t + \hat{\theta}\right)\right] \tag{6}$$

for 31.8 to 32.3 GHz (Ka-band), which is coherently related to the uplink carrier when the loop is in lock (i.e., when $\hat{\theta} \approx \theta$).

The $s_3(t)$ is sampled. The sampling frequency is $4f_0$, derived from the reference generator:

$$\begin{aligned} s_4[m] &= s_3\left(\frac{m}{4f_0}\right) \\ &= \sqrt{P_C}\sin\left(2\pi \times \frac{13}{4}m + \phi\right) \\ &= \sqrt{P_C}\sin\left(\frac{\pi}{2}m + \phi\right) \end{aligned} \tag{7}$$

Associated with $s_4[m]$ is additive, zero-mean, Gaussian noise. A convenient fiction is introduced here: this noise is modeled as white with variance N_0/T_0, where

$$T_0 = \frac{1}{f_0} \tag{8}$$

If the bandpass filter preceding the analog-to-digital converter had a rectangular passband with bandwidth $2f_0$, the additive noise would really be white with variance N_0/T_0. However, the bandpass filter is narrower and, of course, not rectangular. (No analog filter can achieve a perfectly rectangular shape.) Nevertheless, the fictitious model can be justified on the following grounds. When, in subsequent stages of processing, the noise is lowpass filtered (for example, accumulated), the model variance at the output of the further stages of processing approaches the correct value, regardless of what has been assumed about the shape of the input noise spectral density in the vicinity of $2f_0$. Furthermore, the fiction greatly simplifies the analysis.

If the discrete-time index m in Eq. (7) is replaced successively by 0, 1, 2, and 3, $s[m]$ is found to equal $\sqrt{P_C}\sin\phi$, $\sqrt{P_C}\cos\phi$, $-\sqrt{P_C}\sin\phi$, and $-\sqrt{P_C}\cos\phi$, respectively. The first operation in the digital signal processing is to invert the third and fourth samples out of every group of four. This is followed by a two-way demultiplexing, so that the first and inverted third samples of each group of four are sent down one line and the second and inverted fourth samples go down a different line. In this way, the quadrature-phase (Q) samples and in-phase (I) samples are produced. The Q samples (at a sample rate of $2f_0$) are

$$\sqrt{P_C}\sin\phi + \sqrt{\frac{N_0}{T_0}} \times n_1^{(Q)}$$

where $n_1^{(Q)}$ is a unit-variance, white, Gaussian noise process, an implicit function of time. The I samples (at a sample rate of $2f_0$) are

$$\sqrt{P_C}\cos\phi + \sqrt{\frac{N_0}{T_0}} \times n_1^{(I)}$$

where $n_1^{(I)}$ is a unit-variance, white, Gaussian noise process.

Automatic gain control (AGC) is effected as explained here. M consecutive Q samples are accumulated,

$$M\sqrt{P_C}\sin\phi + \sqrt{M\frac{N_0}{T_0}} \times n_1^{(\Sigma Q)}$$

and M consecutive I samples are accumulated,

$$M\sqrt{P_C}\cos\phi + \sqrt{M\frac{N_0}{T_0}} \times n_1^{(\Sigma I)}$$

where

$$M = 2^{11} \tag{9}$$

Both $n_1^{(\Sigma Q)}$ and $n_1^{(\Sigma I)}$ are independent, unit-variance, white, Gaussian noise processes. Each of these two accumulations is squared, and the two squared accumulations are added together. The expected value of the result is

$$M^2 P_C + 2M \times \frac{N_0}{T_0}$$

The reciprocal of the square root of this measurement is used to produce an AGC scaling factor,

$$\frac{\frac{MT_0}{2T_U}}{\sqrt{M^2 P_C + 2M \times \frac{N_0}{T_0}}} = \frac{\frac{T_0}{2T_U}}{\sqrt{P_C + N_0 B_{AGC}}} \tag{10}$$

where

$$B_{AGC} = \frac{2}{MT_0} \tag{11}$$

The numerator of the scaling factor is assumed here to be $MT_0/(2T_U)$; this is a convenient factor because it means that the strong-signal loop-error signal is $1 \times \sin\phi$, as indicated below, and therefore the strong-signal loop gain is lumped entirely in the loop filter. The B_{AGC} is the effective bandwidth of the AGC power measurement. The exact value of f_0 depends on the channel assignment, but f_0 always equals approximately 9.56 MHz. From Eq. (11), B_{AGC} equals approximately 9336 Hz.

The loop-error signal comes from accumulating the original Q samples. The sample period at the output of the loop error accumulator is T_U, so that the accumulation is a sum over $2T_U/T_0$ samples. (This is an approximation, since T_U is not, in general, an integer multiple of $T_0/2$.) The reciprocal of T_0 is known as the update rate. The result of this accumulation is

$$\frac{2T_U}{T_0}\sqrt{P_C}\sin\phi + \sqrt{\frac{N_0}{T_0}\times\frac{2T_U}{T_0}}\times n_1$$

where n_1 is a unit-variance, white, Gaussian noise process. This accumulation is multiplied by the AGC scaling factor of Eq. (10), and the result is

$$\alpha\sin\phi + \sqrt{\frac{1-\alpha^2}{2T_U B_{AGC}}}\times n_1$$

where α is a suppression factor,

$$\alpha = \frac{1}{\sqrt{1+\dfrac{N_0 B_{AGC}}{P_C}}} \tag{12}$$

For large values of signal-to-noise ratio in the bandwidth B_{AGC}, $\alpha \approx 1$; this is the so-called strong-signal case. The scaled loop-error signal goes to the loop filter with transfer function

$$K_1 z^{-1} + K_2 \times \frac{T_U}{z-1}$$

for a perfect integrator and

$$K z^{-1} \times \frac{T_U + \tau_2(z-1)}{T_U + \tau_1(z-1)}$$

for an imperfect integrator, where z is the z-transform variable for a discrete-time system. The strong-signal loop gain is incorporated into the loop filter transfer function.

The STM carrier loop will be part analog and part digital; therefore, it is appropriate to use an s-domain characterization for the closed-loop circuit. To obtain the closed-loop transfer function, it is necessary first to find an s-domain equivalent for the z-domain loop filter transfer function. This can be done by substituting sT_U for $z-1$. The resulting analog-equivalent loop filter transfer function $F(s)$ is

$$F(s) = \begin{cases} \dfrac{K_1 s + K_2}{s} & \text{perfect integrator} \\ K\dfrac{1+\tau_2 s}{1+\tau_1 s} & \text{imperfect integrator} \end{cases} \tag{13}$$

When the carrier loop is in phase lock, $\sin\phi \approx \phi$. The closed-loop transfer function $H(s)$ is

$$H(s) = \frac{\alpha F(s)}{s + \alpha F(s)} \tag{14}$$

Combining Eqs. (13) and (14),

$$H(s) = \begin{cases} \dfrac{\alpha K_1 s + \alpha K_2}{s^2 + \alpha K_1 s + \alpha K_2} & \text{perfect integrator} \\ \dfrac{\alpha K \tau_2 s + \alpha K}{\tau_1 s^2 + (1 + \alpha K \tau_2) s + \alpha K} & \text{imperfect integrator} \end{cases} \tag{15}$$

The (one-sided) noise-equivalent loop bandwidth B_L is [2]

$$B_L = \begin{cases} \dfrac{\alpha K_1^2 + K_2}{4K_1} & \text{perfect integrator} \\ \dfrac{\alpha K \left(\tau_1 + \alpha K \tau_2^2\right)}{4\tau_1 \left(\alpha K \tau_2 + 1\right)} & \text{imperfect integrator} \end{cases} \tag{16}$$

The loop damping factor ζ_L is

$$\zeta_L = \begin{cases} \dfrac{K_1}{2}\sqrt{\dfrac{\alpha}{K_2}} & \text{perfect integrator} \\ \dfrac{1 + \alpha K \tau_2}{2\sqrt{\alpha K \tau_1}} & \text{imperfect integrator} \end{cases} \tag{17}$$

The B_L and ζ_L are not constants: these performance parameters are (through α) functions of P_C/N_0. The variation of B_L with P_C/N_0 is a desirable property in space transponders. At strong-signal ($\alpha = 1$), the loop bandwidth takes on a design value that is appropriate most of the time; this value is denoted B_{LS}. When P_C/N_0 is relatively small, the loop bandwidth narrows. This is an adaptive feature; it means a sacrifice of some tracking performance for an improved signal-to-noise ratio [3]. The minimum value of B_L occurs at carrier threshold, and this minimum value is denoted B_{L0}. It is customary in receiver specifications to quote twice B_{L0} (that is, $2B_{L0}$), rather than B_{L0}. The loop-damping factor also varies between a minimum ζ_{L0} at the carrier threshold and a maximum ζ_{LS} at the strong signal.

A loop with a perfect integrator is characterized by the two parameters K_1 and K_2. A loop with an imperfect integrator is characterized by the strong-signal loop gain K and the time-constant parameters τ_1 and τ_2. (B_{AGC} also plays a role, but it has a fixed value for STM.) There will be great flexibility in selecting these important parameters. In this article, however, only four representative loops are considered. Table 1 shows these four. Loop L_2 has imperfect integration and parameter values to match those of the X-band Deep Space Transponder (DST) used by Cassini [4]. (However, B_{AGC} is not the same for the STM and the DST, so L_2 and the DST do not have exactly the same loop bandwidths and damping factors.) Loop L_1 has perfect integration; its parameters were chosen to yield comparable loop bandwidths and damping factors as for L_2. (But the tracking performance of L_1 will be better because of the perfect integration.) Loop L_3, which has perfect integration, and L_4, which has imperfect integration, have loop bandwidths that are comparable with each other but which are significantly larger than those for L_1 and L_2.

Table 1. Four carrier loops with parameters.

Carrier loop	Integration	Parameters	B_{AGC}, Hz	$2B_{L0}$, Hz	B_{LS}, Hz	ζ_{L0}	ζ_{LS}
L_1	Perfect	$K_1 = 342$ $K_2 = 6190$	9336	16	90	0.44	2.17
L_2	Imperfect	$K = 2.2 \times 10^7$ $\tau_1 = 3556$ $\tau_2 = 0.0556$	9336	16	90	0.45	2.19
L_3	Perfect	$K_1 = 760$ $K_2 = 30,600$	9336	47	200	0.58	2.17
L_4	Imperfect	$K = 3.0 \times 10^7$ $\tau_1 = 1000$ $\tau_2 = 0.025$	9336	46	200	0.57	2.17

III. Best-Lock Frequency Drift in an Idling Carrier Loop

When the receiver idles, so that noise alone is at the loop input, $P_C = 0$, and this implies $\alpha = 0$. The input to the loop filter is then

$$\sqrt{\frac{1}{2T_U B_{AGC}}} \times n_1$$

That is to say, the input to the loop filter is white, Gaussian, discrete-time noise with variance $1/(2T_U B_{AGC})$.

In the case of perfect integration, it is possible to calculate the root-mean-square (rms) frequency offset as a function of time since loss of lock. If $x[k]$ denotes the discrete-time input to the loop filter and $y[k]$ the output, then for this case,

$$y[k] = K_1 x[k-1] + K_2 T_U \sum_{i=0}^{k-1} x[i] \tag{18}$$

The $x[k]$ are independent, each with a mean of zero and a variance of $1/(2T_U B_{AGC})$. The standard deviation of $y[k]$ is

$$\sigma_y = \sqrt{\left(\frac{K_1^2 + 2K_1 K_2 T_U}{2T_U B_{AGC}}\right) + \left(\frac{K_2^2}{2B_{AGC}}\right) t} \tag{19}$$

where t is the time since loss of lock, $t = kT_U$. The rms frequency offset, in hertz, is

$$\frac{1}{2\pi}\sigma_y$$

In the case of imperfect integration, no such simple solution for the rms frequency offset exists, but the action of the loop filter is easily simulated. The output of the loop filter is an angular frequency, representing an offset in the best-lock angular frequency of the idling loop. A computer program was

written to produce this loop filter output. A random number generator was used to produce sample input noise having the proper statistics. The loop filter output was divided by 2π to get cyclical frequency (i.e., units of hertz). A T_U^{-1} of 75,000 was used. The corresponding rms frequency offset was calculated using a sample size of 10, and it is shown in Fig. 2 as a function of time since loss of lock.

For the loops with perfect integration (L_1 and L_3), the rms best-lock frequency offset grows with time. For the loops with imperfect integration (L_2 and L_4), the rms best-lock frequency offset does not grow significantly. Thus, the loops with imperfect integration have an advantage. After many hours of idling, L_2 and L_4 can be acquired more quickly when a new signal arrives than can their counterparts with perfect integration.

It must be remembered, though, that there are other factors, like temperature variation, that cause best-lock frequency drift. So, in some circumstances, the effect of thermal noise on an idling carrier loop may not be the dominant factor in determining the rms best-lock frequency offset.

IV. Flexible Loop Filter Implementation

The previous sections have demonstrated that the choice between perfect and imperfect integration depends on the relative importance of minimizing best-lock frequency drift and maximizing tracking performance. A flexible loop filter structure that can be configured for either perfect or imperfect integration would be the best solution for the STM. Figure 3 is just such a structure. In that figure, the final delay element represents the transport delay of the loop.

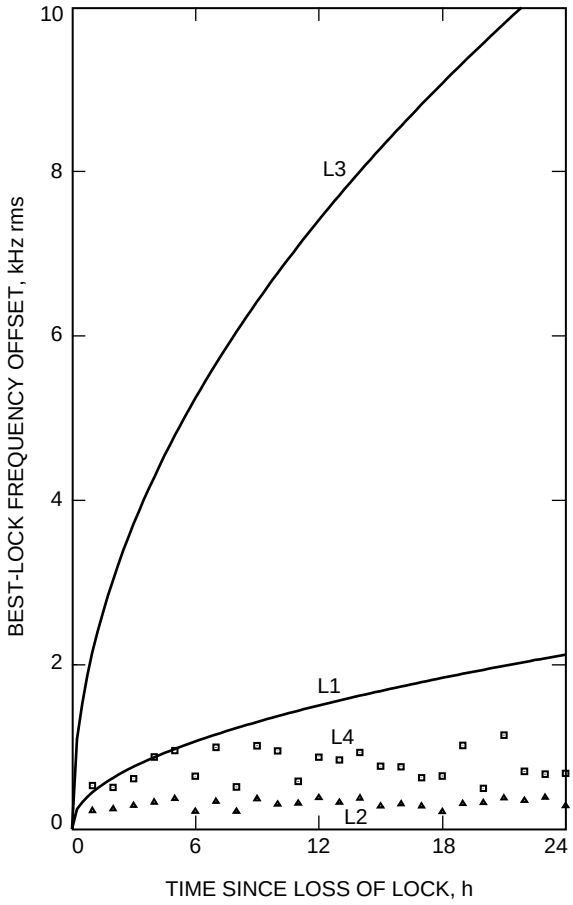

Fig. 2. Best-lock frequency offset versus time since loss of lock.

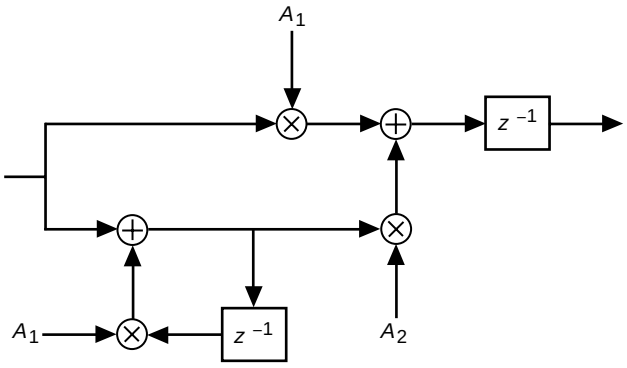

Fig. 3. Loop filter implementation.

The transfer function of the loop filter shown in Fig. 3 is given by

$$A_1 z^{-1} + \frac{A_2}{z - A_3}$$

This transfer function represents a perfect integrator when

$$\left.\begin{aligned} A_1 &= K_1 \\ A_2 &= K_2 T_U \\ A_3 &= 1 \end{aligned}\right\} \tag{20}$$

Alternatively, the general transfer function for the implementation of Fig. 3 may be put in the form

$$z^{-1}\left[\frac{\tau_1(A_1 + A_2 - A_1 A_3) + \tau_1(A_1 + A_2)(z-1)}{\tau_1(1 - A_3) + \tau_1(z-1)}\right]$$

This matches the form of an imperfect integrator when

$$\left.\begin{aligned} \tau_1(1 - A_3) &= T_U \\ \tau_1(A_1 + A_2) &= K\tau_2 \\ \tau_1(A_1 + A_2 - A_1 A_3) &= K T_U \end{aligned}\right\} \tag{21}$$

Solving for the parameters A_1, A_2, and A_3 gives

$$\left.\begin{aligned} A_1 &= K\frac{T_U-\tau_2}{T_U-\tau_1} \\ A_2 &= K\left[\frac{\tau_2}{\tau_1}-\frac{T_U-\tau_2}{T_U-\tau_1}\right] \\ A_3 &= 1-\frac{T_U}{\tau_1} \end{aligned}\right\} \tag{22}$$

Hence, the one loop filter structure shown in Fig. 3 produces a perfect integrator when the parameters A_1, A_2, and A_3 are assigned the values given in Eq. (20). When, instead, the parameters are assigned values according to Eq. (22), an imperfect integrator is effected.

Table 2 shows the appropriate values of A_1, A_2, and A_3 for each of the carrier loops considered in this article. The values given in this table are based on the assumption that $T_U^{-1} = 75,000$ Hz. A few comments are in order about the precision with which the parameters should be set. The A_1 and A_2 are not critical. A precision of about ± 1 percent is adequate for these two parameters. The loop design is quite sensitive, however, to the value of A_3. This can best be seen by considering the required value of A_3 for each of the four loop designs considered in this article. For the perfect integrators L_1 and L_3, A_3 should equal *exactly* 1; this is, of course, easily implemented with a bypass of the multiplication. For the imperfect integrators L_2 and L_4, A_3 needs to be a value that equals 1 minus a small, precise amount,

$$A_3 = 1-\epsilon \tag{23}$$

where

$$\epsilon = \begin{cases} 3.750\times 10^{-9} & L_2 \\ 1.333\times 10^{-8} & L_4 \end{cases} \tag{24}$$

The ϵ should be set with a precision of about ± 1 percent in order to get a precision of about ± 1 percent on B_L.

Table 2. A_1, A_2, and A_3 for the four carrier loops considered in this article with $T_U^{-1} = 7500$.

Carrier loop	A_1	A_2	A_3
L_1	342.0	0.0825	1.00000000000
L_2	343.9	0.0825	0.99999999625
L_3	760.0	0.4080	1.00000000000
L_4	749.6	0.4000	0.99999998666

V. Conclusions

The best-lock frequency of an idling carrier loop will drift in response to thermal noise at the receiver input. This drift is much worse for a (second-order) loop with a perfect integrator than it is for one with an imperfect integrator. On the other hand, a loop with a perfect integrator offers better tracking performance. STM features a flexible loop filter design that accommodates both types of loops.

References

[1] A. J. Viterbi, *Principles of Coherent Communication*, New York: McGraw-Hill, 1966.

[2] S. A. Stephens and J. B. Thomas, "Controlled-Root Formulation for Digital Phase-Locked Loops," *IEEE Transactions on Aerospace and Electronic Systems*, vol. 31, no. 1, pp. 78–95, January 1995.

[3] R. M. Jaffe and E. Rechtin, "Design and Performance of Phase-Lock Circuits Capable of Near Optimum Performance Over a Wide Range of Input Signals and Noise Levels," *IRE Transactions on Information Theory*, vol. IT-1, pp. 67–76, March 1955.

[4] N. R. Mysoor, J. D. Perret, and A. W. Kermode, "An X-Band Spacecraft Transponder for Deep Space Applications—Design Concepts and Breadboard Performance," *IEEE Transactions on Microwave Theory and Techniques*, vol. 40, no. 6, pp. 1192–1197, June 1992.